ELSEVIER

Composites: Part A 30 (1999) 147–152

composites
Part A: applied science and manufacturing

Biaxial testing of high strength carbon fiber composite cylinders for pulsed magnet reinforcement

N Bednar*, H Garmestani

National High Magnetic Field Laboratory, Tallahassee, FL, USA

Abstract

A methodology is introduced to test carbon-fiber-reinforced, hoop-wound composite cylinders for their biaxial mechanical properties under axial compression and hoop tension. The understanding of the behavior of these composites under biaxial loads is extremely important in the design of pulsed magnets. These composites are used as reinforcements for both the inner conducting layers and as an overall exterior reinforcement. Testing of actual pulsed magnets to ascertain design change effects of composite reinforcement schemes on the maximum attainable field can be expensive; hence, a standard biaxial testing method is desirable which is relevant to the design of pulsed magnets. In this investigation, an attempt was made to produce a standard testing procedure aimed at measuring the biaxial mechanical properties (elastic, plastic, and failure envelope) of composite materials. This methodology was applied to two different carbon/epoxy based composites. The results of these tests (elastic properties and failure points) are compared with theoretical predictions, specifically those due to Tsai-Wu.

Keywords: A. Carbon fiber; Magnet reinforcement

1. Introduction

Pulsed magnet reinforcement has taken many forms in the past, with composite materials being of particular interest for their very high tensile strength to mass ratio. The high strength to mass ratio is amenable to pulse magnet reinforcement because a low thermal mass and low heat capacity can afford a quick dissipation of internal heat generated by the electrical current and hence allow longer pulses or a greater frequency of them.

Of importance to magnet designers is a complete and accurate description of each of the layered materials in the magnet. The composite shell has previously been much more difficult to characterize due to its anisotropy and brittle nature and because its failure will be under a state of biaxial or even triaxial stress. Frequently, composite materials require special testing fixtures for biaxial testing, and the specimens must often be tailor-made for the particular test. Additionally, few standards exist for the biaxial characterization of fiber/epoxy composites.

Examples of investigations into the characterization of composite cylinders under biaxial stress exist in the literature, although many focus on laminated cylinders with multi-axial windings [1]. Some of these composites fall into the quasi-isotropic group, which are quite different form the uniaxially wound specimens in this investigation. Remaining examples include differing types of fiber material such as aramid or E-glass. Published reports on biaxial testing of composites, specifically carbon based, are few. Interestingly, the methods of testing the specimens are quite varied. Highton and Adeoye [2] used a method of internal pressure and axial compression, which included different setups for different testing modes. For the case of pure hoop stress, they used endplugs with O-rings, with the endplugs transferring load from the hydraulic fluid in the axial direction directly to the uniaxial test machine. Several others had setups such as this. For example, Swanson and Trask's experimental setup for testing cylinders under biaxial stress included an internal aluminum plug which reduced the volume of hydraulic fluid required and which was secured to the endplugs, reacting the axial load directly to the testing machine [3]. The work at the National High Magnetic Field Laboratory included attempts at using O-rings, but they were unsuccessful. For this reason, an alternative method of sealing and direct pressurization of the specimen was carried out.

Work by Pernambuco-Wise et al. offers another interesting method of investigating the mechanical strength of composite cylinders for pulse magnet reinforcement in situ [4]. Small 'firecracker' magnets are manufactured with differing thicknesses of composite material for external reinforcement. The magnets are then energized to failure,

* Corresponding author

1359-835X/99/$ - see front matter © 1998 Published by Elsevier Science Ltd. All rights reserved.
PII: S1359-835X(98)00101-8

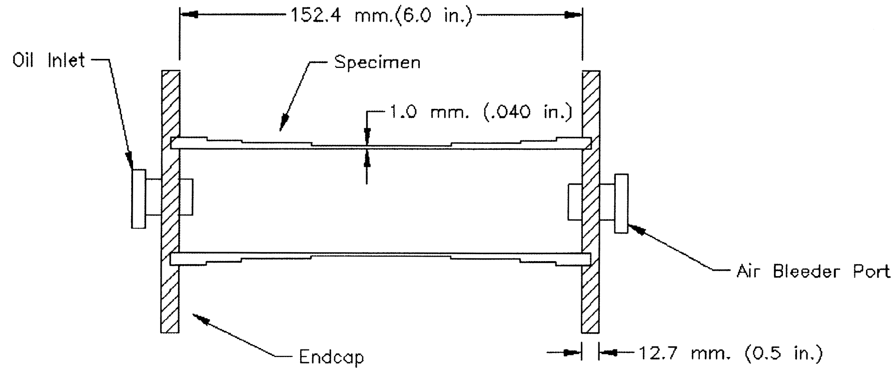

Fig. 1. Schematic of cylindrical composite specimen with endcaps.

and the effectiveness of different reinforcing schemes is determined. Although the method is for purposes of comparison and does not directly measure the failure strengths, it allows for the measurement of ultimate allowable magnetic field based on given composite dimensions. The present investigation is not limited to pulse magnet applications. The methodology introduced here will be applicable to other fields of mechanics where biaxial properties are of interest.

2. Theoretical analysis

The composite reinforcing shell of a pulsed magnet is under a biaxial state of stress such that internal radial expansion and axial compression of the magnet can result in a corresponding hoop stress and axial compressive stress in the composite shell. The specimen geometry is cylindrical, and although there has been some question as to the validity of using this geometry for biaxial testing [5], it offers at least three major benefits: (1) cylinders are a more accurate representation of pulsed magnet reinforcement than flat coupons; (2) the cylinders, unlike flat panels, are free from the particular stress concentrations that arise from boundary edges such as those inherently found on flat composite plate specimens; and (3) developing biaxial stress on a flat specimen by means of two separate uniaxial test machines, or by some kind of special fixture, is more difficult than utilizing one uniaxial machine and an internal pressurizing system for cylindrical specimens.

This configuration does, however, introduce a flaw, since the radial stress distribution (and that of circumferential stress) is not uniform through the thickness of the cylinder. There is a transition from $\sigma_r = -P_i$ at the inner radius to $\sigma_r = 0$ at the surface of the cylinder. Since the maximum stress is initiated at the inner radius, it can be assumed that failure starts at the inner radius. However, the small value for the thickness of the wall (1 mm) allows a model of plane stress to be used in the calculations and presumes that the radial stress is negligible relative to stress in the other directions.

The composite specimens were considered as thin-wall pressure vessels with a wall thickness of 1 mm and an internal diameter of 38.1 mm (1.5 in.). The equations describing hoop stress and axial stress in a thin-wall pressure vessel are as follows:

$$\sigma_\theta = \frac{Pr}{t} \tag{1}$$

$$\sigma_z = \frac{Pr}{2t} - \frac{F}{A_c} \tag{2}$$

where P is internal pressure, r is specimen inner radius, and t is average wall thickness. F is the magnitude of the axial force applied to the specimen by the hydraulic actuator, and A_c is the cross-sectional area of the specimen.

The composite specimens in this study were all of the hoop-wound (90° type), and as such can be considered an orthotropic construction with symmetry in the radial and axial directions. Equations describing the elastic response of an orthotropic element in cylindrical coordinates under plane stress are

$$\begin{bmatrix} \sigma_z \\ \sigma_\theta \\ \tau_{z\theta} \end{bmatrix} = \begin{bmatrix} C_{11} & C_{12} & 0 \\ C_{21} & C_{22} & 0 \\ 0 & 0 & C_{66} \end{bmatrix} \begin{bmatrix} \epsilon_z \\ \epsilon_\theta \\ \epsilon_{z\theta} \end{bmatrix} \tag{3}$$

which in the absence of applied shear stress further evolve to

$$\epsilon_z = \frac{\sigma_z}{E_z} - \frac{\nu_{\theta z}}{E_\theta}\sigma_\theta \tag{4}$$

$$\epsilon_\theta = \frac{\sigma_\theta}{E_\theta} - \frac{\nu_{z\theta}}{E_z}\sigma_z \tag{5}$$

By performing separate tests on each specimen under which first $\sigma_\theta = 0$ and $\sigma_z < 0$, and then $\sigma_z = 0$ and $\sigma_\theta > 0$, both the elastic moduli E_θ and E_z, and Poisson ratios $\nu_{z\theta}$ and $\nu_{\theta z}$ can be measured. Further applications of stress to the point of failure gives the maximum axial stress and maximum circumferential stress at a particular ratio of the two.

Table 1
Experimental results of mechanical tests on two different kinds of cylindrical composite specimens (ksi)

(a) NHMFL	E_θ	E_z	$\nu_{\theta z}$	$\sigma_{\theta max}$	σ_{zmin}	*s*	Failure mode
1126-1							
1016-1	–	–	–	46.0	− 13.1	− 3.5	Axial −
1016-2	–	1940	–	69.0	− 11.9	− 5.8	Axial −
1016-3	–	–	–	96.9	− 2.2	− 44.0	Axial −
09171	–	–	–	79.5	− 9.4	− 8.5	Axial −
09172	–	1924	–	–	–	–	Premature
82901	–	–	–	–	–	–	–
82902	28 300	–	–	0	− 12.9	0	Axial −
remn1	–	–	–	0	− 12.3	0	Axial −
remn2	–	–		0	− 14.5	0	Axial −
0528-1	–	1944		0	− 12.6	0	Axial −

(b) Spyro-Tech	E_θ	E_z	$\nu_{z\theta}$	$\sigma_{\theta max}$	σ_{zmin}	*s*	Failure mode
1114-1	–	–	–	9.7	2.5	3.9	Axial +
1114-2	26 880	1800	0.250	89.3	− 19.1	− 4.7	Hoop
1114-3	25 870	1796	0.285	–	–	–	Premature
1114-4	29 770	1840	0.285	94.5	− 18.5	− 5.2	Combined
1114-5	28 300	1818	0.230	–	–	–	Premature
1114-6	–	1862	–	–	− 13.9	0	Axial −

This ratio is defined as

$$S = \frac{\sigma_\theta}{\sigma_z} \quad (6)$$

3. Experimental set-up

The specimen is a hoop-wound composite with reinforced ends (Fig. 1). The internal diameter is 1.50 in., and the wall thickness is approximately 0.04 in. (1 mm). The overall length of each specimen is 6.0 in. There were a few initial designs that included specimens 12.0 in. in length, but these were reevaluated due to the occurrence of leaks. Each end had a 0.5-in.-thick G-10 fiberglass endcap with an annular channel 0.25 in. deep. The specimen end was inserted into the channel and secured with a two-part epoxy. Each endcap had a threaded oil inlet and air release port into which a 3/8″ brass bushing was threaded and epoxied.

A critical component of the specimen design was a flexible polyurethane internal bladder which was cast from liquid form onto the inside wall of the specimen. This bladder prohibited the oil from causing premature failure by weepage as seen by others [6]. The polyurethane bladder adhered to the inside of the specimen, also serving to evenly distribute the internal pressure.

Given the particular orientation of the biaxial stresses and the geometry of the specimens, it was realized that for the specimens to fracture within the gage length, they would require reinforcement near the ends. Previous tests on composites [7] showed the importance of reinforcement on specimen ends in promoting a smooth transfer of stress from the ends to the center gage length area. Amaldi and Marchetti [8] and Swanson et al. [9] performed finite element analysis to determine optimal reinforcement schemes for their specimens. The end-region reinforcement of specimens in this investigation followed a similar concept, in that if axial compression of the specimen is to produce failure in the center gage length, the end regions must be sufficiently strong to transitionally transmit the load to the gage length without failure by crushing due to end conditions. Preliminary testing indicated that excess reinforcement beyond a quarter of an inch at the ends would not be required. The configuration of the end-region reinforcement for the specimens was as follows: two inches from each end had four layers of winding, one inch from each end had eight layers of winding, and one-half inch from each end had ten layers of winding. This reinforcement design proved satisfactory, and all valid specimen failure occurred within the gage length.

4. Experimental procedure

Uniaxial, hoop-wound carbon-fiber composite cylinders with an epoxy matrix were tested to failure under varying biaxial stress combinations of axial compression and hoop tension. This was achieved by means of both a 22-kip MTS servo-hydraulic machine and an Enerpac hand pump, which delivered a maximum of 10 ksi. The hand pump was used to internally pressurize the cylinders, thus producing hoop stress and axial tension, the latter of which could be negated by means of sealed endcaps and application of compressive force from the MTS machine. Results of these tests are presented here, including elastic moduli, failure stresses, and failure modes.

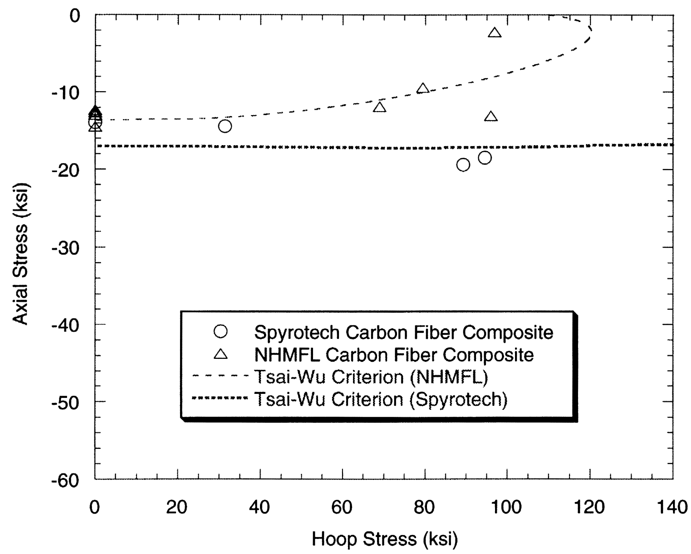

Fig. 2. Graphic representation of hoop stress and axial stress failure envelope.

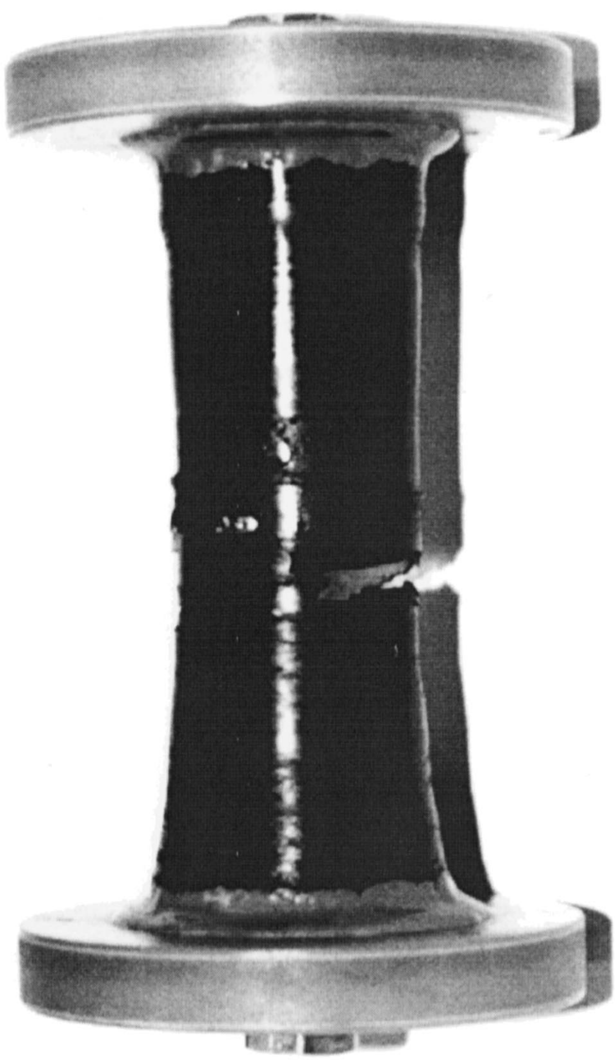

Fig. 3. Example of carbon–epoxy composite hoop failure mode.

For each specimen, three individual tests were performed. First, the specimen was axially compressed to a small fraction of the estimated failure strength (~ 500 lbf.) with a 22-kip MTS servo-hydraulic test machine. This process was performed in the absence of any internal pressure on the specimen, allowing calculation of the transverse elastic modulus and Poisson ratio $\nu_{z\theta}$.

$$\sigma_\theta = 0, \;\; E_z = \frac{\sigma_z}{\epsilon_z}, \;\; \nu_{z\theta} = \frac{\epsilon_z}{\epsilon_\theta} \tag{7}$$

The second process of the experimental procedure was to internally pressurize each specimen via a 10-ksi Enerpac handpump up to an appropriate hoop stress much lower than the estimated failure point, while maintaining an axial compressive force with the MTS machine such that the axial stress in the specimen was nearly zero. The elastic modulus in the fiber direction (hoop direction) and the Poisson ratio $\nu_{z\theta}$ are given as

$$\sigma_{\theta z} = 0, \;\; E_\theta = \frac{\sigma_\theta}{\epsilon_\theta}, \;\; \nu_{\theta z} = \frac{\epsilon_\theta}{\epsilon_z} \tag{8}$$

The final stage of testing was to apply internal pressure at near-zero axial stress and then apply axial compression until failure of the specimen occurred. Failure was typically indicated by a loud sound and a drop in both pressure and axial load. In some cases, a sizable portion of the axial load could be maintained after audible failure of the specimen, although internal pressure decreased abruptly.

5. Experimental results

Specimens from two carbon–epoxy composite materials were tested. The first group was manufactured by the authors at The National High Magnetic Field Laboratory using a wet winding technique. The carbon fibers in this

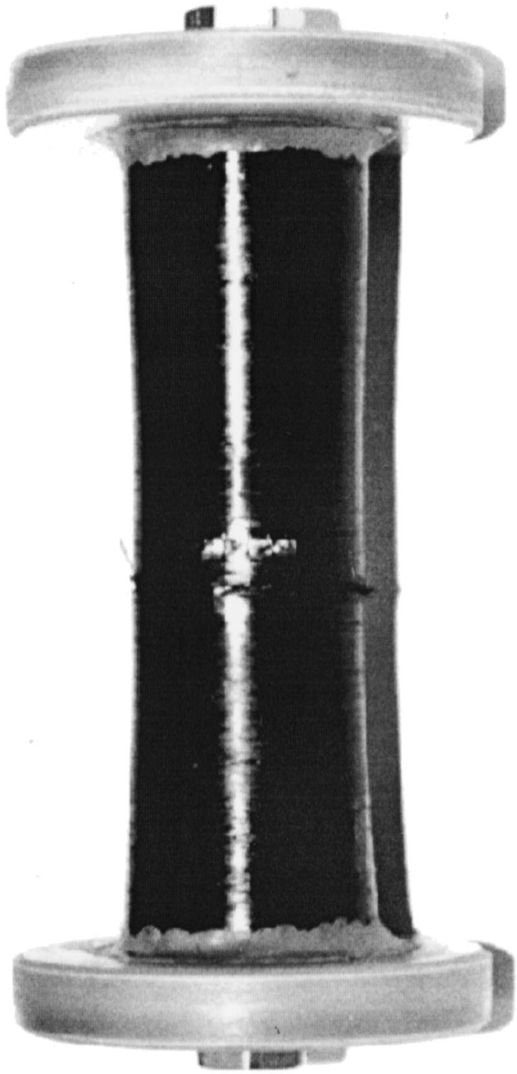

Fig. 4. Example of carbon–epoxy composite axial failure mode.

group were Hercules Magnamite IM8, and the epoxy matrix was CTD 521. The composite specimens in this group were cured overnight at approximately 90°C. The second group of specimens tested were purchased from SpyroTech Inc. of Lincoln, Nebraska. The fibers used for these samples were Voltex Panex carbon fibers, and the epoxy matrix used was Shell 9405-9470. The cure cycle was 82°C for 4 h, then 121°C for another 4 h. Both types of composites were fabricated using a wet-winding technique.

The transverse and hoop elastic moduli as well as the Poisson ratio and failure stresses for various specimens are presented in Table 1.

The specimen design and experimental procedure were characterized by an evolutionary process which is reflected in the presented data. Initial experiments resulted in premature failure due to oil leakage, but failure stresses were measured in a number of other specimens.

Fig. 2 shows a graphic representation of the failure points for a successful set of experiments. There are curves superimposed over each of the two sets of data, using the Tsai-Wu criterion which is explained below.

As explained below, each curve is a fit based on the Tsai-Wu criterion. This is an anisotropic failure that creates an ellipse in the biaxial plane. For strength values that could not be obtained with the current apparatus, information was taken from other published tables. Additionally, the biaxial interaction term was chosen so as to best fit the data.

Investigation of failure modes was an essential component of this research. Global failure patterns and structural observation were the main tools used for this type of analysis. Even well formulated failure criteria often do not specify the particular mode of failure, which can determine a structure's ability to maintain some fraction of the applied load after being damaged. All but two of the specimens had relatively localized axial failure by means of a splitting along the circumference of the cylinder. Two specimens that exhibited either predominant hoop failure or a combination of hoop and axial failure resulted in catastrophic rupturing of the specimen. This was characterized by large open tears parallel to the specimen axis. Fig. 3 shows an example of hoop failure, indicated by missing material and open tears. Fig. 4 indicates an example of axial failure with small areas of crushed material barely visible and very little or no fiber breakage.

6. Failure analysis

There are many failure criteria for composite materials, each of which may be applicable to a particular case. As a result, there may not be a single failure criterion that is universally applicable for all cases. Changes in loading conditions, geometrical uniqueness, and fiber and epoxy characteristics, and the nature of the component interaction can all contribute in some way to alter the ultimate stresses that a composite structure is capable of withstanding. However, it is usually possible to describe the basic nature of the failure envelope for a composite under biaxial loading conditions with a particular mathematical model. These mathematical models are ultimately dependent on the experimental data for their effectiveness in practical applications. In this study, the well known Tsai-Wu failure criterion of anisotropic materials was used to fit the experimental data, which are in relatively good agreement for these specimens. A version of the Tsai-Wu failure criterion is given here in the following form

$$f(\sigma_i) = F_i\sigma_i + F_{ij}\sigma_i\sigma_j = 1 \quad (9)$$

where terms higher than second order are omitted. When a plane stress model is adopted in the absence of applied shear stresses, Eq. (9) can be simplified to the following:

$$A\sigma_\theta^2 + B\sigma_\theta\sigma_z + C\sigma_z^2 + D\sigma_\theta + E\sigma_z = 1 \quad (10)$$

The constants can be extracted as follows. Let $\sigma_c^{'}$ be the transverse compressive failure stress in the absence of internal pressurization, σ_c the transverse tensile stress (taken from published values), σ_t the hoop tensile failure stress in the absence of compressive stress, and σ_t' the hoop compressive stress (also taken form published results). Eq. (10) then results in

$$C = \frac{1}{\sigma_c \sigma_c'} \qquad A = \frac{1}{\sigma_t \sigma_t'} \tag{11}$$

$$E = \left(\frac{1}{\sigma_c} - \frac{1}{\sigma_c'}\right) \qquad D = \left(\frac{1}{\sigma_t} - \frac{1}{\sigma_t'}\right) \tag{12}$$

Also, assume that a state of biaxial failure is achieved at a compressive stress of σ_{cb} and a circumferential stress of σ_{tb}. For this investigation, only the failure envelope in quadrant IV was of concern. So, in terms of the other constants:

$$B = \frac{1}{\sigma_{bc}\sigma_{bt}}\left[1 - \left(\frac{\sigma_{bc}}{\sigma_c}\right)^2 - \left(\frac{\sigma_{bt}}{\sigma_t}\right)^2\right] \tag{13}$$

Difficulties sometimes arose in holding a specimen in a condition of pure hoop stress. Some small axial load inevitably came into and out of the picture due to the deformation of intermediary materials present, such as platens and centering rings. This was accounted for, however, in elastic modulus calculations in a few cases, by analyzing global stress and strain over a region bounded by zero axial stress over time.

7. Discussion

As reinforcement material for pulse magnets, carbon-fiber composites offer one of the highest strength-to-weight ratios of any material. As brittle, anisotropic materials, however, they need to be characterized fully. Here, specimens of two carbon–epoxy materials were mechanically tested to obtain elastic constants and ultimate failure stresses. The elastic moduli of the specimens from both groups were quite similar. Major differences were in the ultimate strengths and failure modes under biaxial stress.

The ultimate strength of a composite in uniaxial tension is generally attributed to the high-strength fibers, with the matrix simply acting as a load distribution system. The failure under biaxial stress is more complicated since there are components of transverse compression, and fiber-axial tension. Fiber strengths are often given in specifications as high as 5 GPa; however, these exceptionally high ultimate strengths are unusual in composite form. The final strengths are determined by a combination of properties of the system of materials, which include both fibers and matrix materials. This is especially true of composites tested under biaxial stress, where failure may be determined by a combination of factors including not only the ultimate strengths of the matrix and fiber, but also fiber–matrix interfacial shear strength and the presence of voids and micro cracks. From this investigation, an important point to be highlighted is the sensitivity of the carbon–epoxy composite materials to transverse stress. Of course, these are uniaxially wound composites, and not laminates; however, these data are valid for a single layer in the 90° direction.

8. Conclusion

A biaxial material testing system for composite cylinders (hoop stress and axial compression) was designed and used to evaluate two different carbon–epoxy based composites. The results indicate that there may be a large variation in biaxial strength with variation in carbon fiber/epoxy selection and cure cycle. It was possible to measure the elastic modulus in both the fiber direction and transverse to the fiber direction (see Table 1(a)), but difficulty was encountered with the Poisson ratio due to the non-uniform pressure loading caused by manual operation of the hand pump. The successful testing to failure of the composites provided a failure envelope within the fourth quadrant of the yield surface. It was also possible to fit the two data sets with curves based on the failure model of the Tsai-Wu criterion. The comparison shows that such a model may be sufficient to characterize the failure history in these two materials. The biaxial fixture design presented here shows promise in standardization of such tests to provide a reproducible set of data for biaxial experiments.

References

[1] Swanson SR, Trask BC. Strength of quasi-isotropic laminates under off-axis loading. Compos Sci Technol 1989;34:19.
[2] Highton J, Adeoye AB, et al. Fracture stresses ± 75 degree filament wound GRP tubes under biaxial loads. J Strain Anal 1985;20(3):140.
[3] Swanson SR, Trask BC. An examination of failure strength in [0/ ± 60] laminates under biaxial stress. Composites 1988;10:400–406.
[4] Pernambuco-Wise P, Rickel DG, et al. Testing of carbon composites using systematic failure of pulse magnets. Internal Report, National High Magnet Field Laboratory, Tallahassee, FL.
[5] Choo VKS, Hull D. Influence of radial compressive stress owing to pressure on the failure modes of composite tube specimens. J Compos Mater 1983;17:356.
[6] Soden PD, Kitching R, et al. Influence of winding angle on the strength and deformation of filament wound composite tubes subjected to uniaxial and biaxial loads. Compos Sci Technol 1993;46:365.
[7] Guess TR. Biaxial testing of composite cylinders: experimental–theoretical comparison. Composites 1980;11:140.
[8] Amaldi A, Marchetti M. Mechanical behavior of filament wound carbon fibre reinforced epoxy resin tubes. 3rd Int Conf Comput Aided Des Campos Mater Technol CADcomp 92, Computational Mechanics, Southampton, 1992, pp. 79–88.
[9] Swanson SR, Messick MJ, Tian Z. Failure of carbon/epoxy lamina under combined stress. J Compos Mater 1987;21:621.